Published OnlineFirst February 20, 2012; DOI:10.1158/0008-5472.CAN-11-2663

Cancer Research

miRNA Signatures Associate with Pathogenesis and Progression of Osteosarcoma

Kevin B. Jones, Zaidoun Salah, Sara Del Mare, et al.

Cancer Res 2012;72:1865-1877. Published OnlineFirst February 20, 2012.

Published OnlineFirst February 20, 2012; DOI:10.1158/0008-5472.CAN-11-2663

Tumor and Stem Cell Biology

Cancer Research

miRNA Signatures Associate with Pathogenesis and Progression of Osteosarcoma

Kevin B. Jones[1], Zaidoun Salah[2], Sara Del Mare[2,3], Marco Galasso[5], Eugenio Gaudio[3], Gerard J. Nuovo[4], Francesca Lovat[3], Kimberly LeBlanc[6], Jeff Palatini[3], R. Lor Randall[1], Stefano Volinia[3,5], Gary S. Stein[6], Carlo M. Croce[3], Jane B. Lian[6], and Rami I. Aqeilan[2,3]

Abstract

Osteosarcoma remains a leading cause of cancer death in adolescents. Treatment paradigms and survival rates have not improved in two decades. Driving the lack of therapeutic inroads, the molecular etiology of osteosarcoma remains elusive. MicroRNAs (miRNAs) have demonstrated far-reaching effects on the cellular biology of development and cancer. Their role in osteosarcomagenesis remains largely unexplored. Here we identify for the first time an miRNA signature reflecting the pathogenesis of osteosarcoma from surgically procured samples from human patients. The signature includes high expression of *miR-181a*, *miR-181b*, and *miR-181c* as well as reduced expression of *miR-16*, *miR-29b*, and *miR-142-5p*. We also demonstrate that *miR-181b* and *miR-29b* exhibit restricted expression to distinct cell populations in the tumor tissue. Further, higher expression of *miR-27a* and *miR-181c** in pre-treatment biopsy samples characterized patients who developed clinical metastatic disease. In addition, higher expression of *miR-451* and *miR-15b* in pre-treatment samples correlated with subsequent positive response to chemotherapy. *In vitro* and *in vivo* functional validation in osteosarcoma cell lines confirmed the tumor suppressive role of *miR-16* and the pro-metastatic role of *miR-27a*. Furthermore, predicted target genes for *miR-16* and *miR-27a* were confirmed as down-regulated by real-time PCR. Affymetrix array profiling of cDNAs from the osteosarcoma specimens and controls were interrogated according to predicted targets of *miR-16*, *miR142-5p*, *miR-29b*, *miR-181a/b*, and *miR-27a*. This analysis revealed positive and negative correlations highlighting pathways of known importance to osteosarcoma, as well as novel genes. Thus, our findings establish a miRNA signature associated with pathogenesis of osteosarcoma as well as critical pre-treatment biomarkers of metastasis and responsiveness to therapy. *Cancer Res; 72(7); 1865–77. ©2012 AACR.*

Introduction

Osteosarcoma (OS) is the most common primary sarcoma of bone and a leading cause of cancer death among adolescents and young adults (1). The cellular events that initiate and propagate osteosarcomagenesis remain poorly understood (2). Most OSs (approximately 90%) are termed "conventional" and have osteoblastic and/or fibroblastic histologic patterns with consistently high-grade nuclear morphologies. Two common alternate histologic subtypes, chondroblastic, characterized by cartilaginous tissues in the tumor, and telangiectatic, characterized by abundant vascular and cystic spaces in the tumor, are also often high grade. When these other subtypes are high grade, they are treated with conventional OS treatment regimens (3).

The genetic and cytogenetic complexity intrinsic to OS make deciphering the origins of its very patterned clinical phenotype especially difficult. Inability to determine which, among the many genetic derangements present in OS, such as aneuploidy, rampant mutations, and manifold copy number variations, are causative of and which are resultant from oncogenic transformation remains a major impediment to progress in understanding its etiology (2). Nonetheless, the consistent clinical pattern of osteosarcomagenesis, characterized by rapid onset of high-grade neoplasms in young people, suggests that some yet undetected, but consistent etiologic event or group of events defines the neoplasm.

miRNAs are short noncoding RNAs that posttranscriptionally modify gene expression in eukaryotic cells. Expression of a

Authors' Affiliations: [1]Department of Orthopaedics and Center for Children's Cancer Research, Huntsman Cancer Institute, University of Utah, Salt Lake City, Utah; [2]Lautenberg Center for Immunology and Cancer Research, IMRIC, Hebrew University-Hadassah Medical School, Jerusalem, Israel; Departments of [3]Molecular Virology, Immunology and Medical Genetics and [4]Pathology, Comprehensive Cancer Center, Ohio State University, Columbus, Ohio; [5]Department of Morphology and Embryology, Data Mining for Analysis of Microarrays, Università degli Studi, Ferrara, Italy; and [6]Department of Cell Biology and Cancer Center, University of Massachusetts Medical School, Worcester, Massachusetts

Note: Supplementary data for this article are available at Cancer Research Online (http://cancerres.aacrjournals.org/).

K.B. Jones and Z. Salah are first coauthors.

Corresponding Authors: Rami I. Aqeilan, Lautenberg Center, Hebrew University, P.O. Box 12272, Jerusalem-91120, Israel. Phone: 9722-6758609; Fax: 9722-6424653; E-mail: aqeilan@cc.huji.ac.il; and Kevin B. Jones, 2000 Circle of Hope Drive, Room 4263, Salt Lake City, Utah-84112. E-mail: kevin.jones@hci.utah.edu

doi: 10.1158/0008-5472.CAN-11-2663

Published OnlineFirst February 20, 2012; DOI:10.1158/0008-5472.CAN-11-2663

single miRNA can silence a large number of genes, granting these molecules extensive control over many cellular functions (4). Knowledge of individual miRNAs effecting developmental biology, cellular differentiation programs, and oncogenesis continues to grow (reviewed in ref. 5). Although specific miRNAs have been functionally evaluated in a few OS cell lines (6–9), and miRNA expression profiled in formalin-fixed, paraffin-embedded OS specimens (10), high quality total RNA from primary OS tissues has been collected prospectively in few centers (11). Appreciating the vast effects possible from oncogenic and other miRNAs, we surveyed a well-characterized group of OSs with array-based technologies. Differential expression profiles were validated with quantitative reverse transcriptase PCR (qRT-PCR), *in situ* hybridization, and functional validation in human OS cell lines both *in vitro* and *in vivo*. Our studies have shown profiles including differential expression of oncogenic and tumor suppressor miRNAs, reflecting OS status.

Materials and Methods

Patients, sample procurement, and isolation of total RNA

With approval of the Institutional Review Board and in compliance with all legal and ethical considerations for human subject research, patients presenting with suspected sarcomas and scheduled for incisional biopsies provided informed consent to have their tissue banked for RNA extraction. Specimens were obtained during these open surgical biopsies, gently washed with normal saline to remove excess blood, and placed immediately into RNAlater (Ambion) by the surgeon. Specimens were kept at 4°C in RNAlater for up to 1 week, then stored at −80°C. When formal pathologic interpretation of histology from other portions of the biopsy specimen rendered a diagnosis of OS, the RNA-preserving tissue specimens were banked and annotated. In preparation for these specific experiments, total RNA was extracted from banked specimens with the TRIzol reagent and method (Invitrogen). Control samples were derived from to-be-discarded bone fragments obtained from similarly consented patients undergoing debridement surgeries for acute, traumatic injuries to the long bones.

Microarray profiling of miRNA and mRNA expression

miRNA microarray was conducted as previously described (12). The integrity of these total RNAs was assessed with an Agilent 2100 bioanalyzer. Total RNA (5 μg) was hybridized on the custom microarray chip (OSUCCC miRNA microchip, version 3.0). This array contains approximately 1,100 probes (including 345 human and 249 mouse miRNA genes spotted in duplicate). Normalized microarray data were managed and analyzed by BRB-ArrayTools, version 3.8.1 (13). Genes whose expression differed by at least 1.5-fold from the median, in at least 20% of the arrays were used. A stringent significance threshold was used to limit the number of false positive findings. The result of this approach was determined by 2 sample *t* test with nominal significance level at 0.01. The false discovery rate (FDR) is the expected proportion of positive results that are false positives at the various levels of significance and was controlled using the step-up method of Benjamini and Hochberg. In this analysis, at any selected FDR level, the expected proportion of false positives was determined. Class prediction algorithms determined whether miRNA expression patterns could accurately differentiate between OS samples and normal human bone controls. We developed models based on the compound covariate predictor, nearest neighbor classification, and support vector machine. The models incorporated genes that were differentially expressed among genes at the significance level (0.05) as assessed by the random variance *t* test. We used the prediction test to identify the classifier signature with the lowest misclassification error.

For the mRNA profiling, 14 of the cohort's OS and 4 of the control samples were hybridized with the Affymetrix Human Genome U133 Plus 2.0 Array. The CEL files were imported and robust multi-array averaging normalized. Genes whose expression differed by at least 1.5-fold from the median in at least 20% of the arrays were used. We carried out class comparisons algorithms in BRB-ArrayTools with the paired *t* test ($P < 0.05$). The union of the target mRNAs was used as an input to DAVID EASE, using the David Bioinformatics Resources system (http://david.abcc.ncifcrf.gov). We compared the list of terms related to the predicted targeted mRNAs. The terms were evaluated by *P* value ($P < 0.05$) and Benjamini–Hochberg correction for multiple testing controlled the *P* values. Target genes selection was carried out by Target Scan software. We evaluated Gene Ontology (http://www.geneontology.org/) and PATHWAY (http://www.genome.jp/kegg/) terms.

RT-PCR validation

TaqMan miRNA assays were used to detect and quantify mature miRNAs as previously described (14) using ABI Prism 7900HT sequence detection systems (Applied Biosystems). Normalization was carried out with RNA *U6*. Samples were run in triplicate, including no-template controls. Relative expression was calculated by the comparative C_t method. qRT-PCR to confirm expression levels in cell lines following transfection with lentiviral vectors was carried out according to a previously described protocol (15). Primers used are noted Supplementary Table S6.

In situ hybridization

Detection of miRNAs by *in situ* hybridization was conducted as previously published (16, 17). Locked nucleic acid (LNA)-modified probes were 5′ labeled with digoxigenin (Exiqon). After protease digestion to expose the target, 2 pmoles/μL of the probe was hybridized to the tissue section for 15 hours, then subjected to a low stringency wash. The probe-target complex was visualized by alkaline phosphatase activity on the chromogen nitroblue tetrazolium and bromochloroindolyl phosphate (Roche Diagnostics) after nuclear fast red counterstain. Coexpression analyses was conducted with the Nuance system as previously published (17).

Cell lines and cell culture

Cell lines (HOS, KHOS, SaOS2, U2OS, and MG-63) were obtained from the American Type Culture Collection and hOB from PromoCell. LM7 is a gift from Dr. Dennis Hughes (The University of Texas MD Anderson). Each line was authenticated

Published OnlineFirst February 20, 2012; DOI:10.1158/0008-5472.CAN-11-2663

as to genotype and phenotype by the source company. Cells were used at low passage for experiments, always less than 6 months of passaging postprocurement.

In vitro viral transduction

Lenti-*miR-16* was a gift from Dr. Yinon Ben-Neriah (Hebrew University, Jerusalem) and Lenti-*miR-27a* was described elsewhere (18). HEK293 cells with *pCMV-VSVG* and *pHR82R* packaging plasmids were used to produce the lenti-miRs. OS cells at subconfluent density (70%) were incubated with the lentivirus for 4 to 5 hours. Selection with 0.5 μg/mL puromycin began the next day. Stable clones were then isolated and verified by qRT-PCR and GFP fluorescence.

Cell proliferation analysis

Cells (1.5×10^3) were plated in 96-well plate and analyzed by a 2,3-bis[2-methoxy-4-nitro-S-sulfophenynl]H-tetrazolium-5 carboxanilide inner salt (XTT) proliferation assay according to the manufacturer's instructions.

Colony formation assay

Cells were plated at a density of 500 cells per well in a 6-well plate in triplicate. After 1 to 2 weeks, the cells were fixed with 70% ethanol, stained with Giemsa and counted.

Matrigel invasion assay

Blind well chemotaxis chambers with 13 mm diameter filters were used for this assay. Polyvinylpyrrolidone-free polycarbonate filters, 8-μm pore size (Costar Scientific Co.), were coated with basement membrane Matrigel (25 μg/filter). Cells (2×10^5) suspended in Dulbecco's Modified Eagle's Medium containing 0.1% bovine serum albumin were added to the upper chamber. Conditioned medium of NIH3T3 fibroblasts was placed in the lower chamber. Assays were carried out at 37°C in 5% CO_2. More than 90% of the cells attached to the filter after incubation for 7 hours. After incubation, the upper surface of the filter was freed of cells with a cotton swab. Cells that passed through the filter to bottom side were fixed with methanol and stained with Giemsa. Each triplicate assay was conducted twice. Invasive cells were counted in 10 representative light microscopy fields.

Mouse experiments

All animals were housed in the Hebrew University animal facility and the experiments with live animals were approved by our institute animal committee and conducted in accordance with NIH guidelines. HOS cells expressing miR-control, *miR16*, or *miR-27a* were injected s.c. (5×10^6 cells) or i.v. (1×10^6 cells), respectively, into nonobese diabetic/severe combined immunodeficient (NOD/SCID) mice. For SC experiments, tumor volume was evaluated weekly and tumor mass measured at the end of the experiment. For i.v. experiments, 6 weeks after injecting cells expressing *miR-27a*-GFP or control-*miR*-GFP, mice were sacrificed and lungs as well as legs and forearms were examined for micro- and macrometastases, respectively, using a fluorescent stereomicroscope (Olympus).

Immunohistochemistry

Immunohistochemistry was carried out on formalin-fixed, paraffin-embedded specimens with the following antibodies: polyclonal antiactive caspase-3 (Cell Signaling; dilution 1:100), polyclonal anti-BCL2 (Abcam ab7973-1; dilution 1:100), and polyclonal anti-NFAT5 (Abcam ab110995; dilution 1:100). Detection was carried out by ABC kit (BA-1000, VECTOR Laboratories) according to manufacturer's specifications. Slides were reviewed in blinded fashion and ranked according to density of immunostain. Five bone marrow core biopsy controls were used, assessing immunostaining on trabecular bone rimming osteoblasts.

Results

miRNA expression signature for osteosarcomagenesis

To identify differentially expressed miRNAs common in osteosarcomagenesis, we compared miRNA expression profiles from 18 pretreatment biopsy samples from conventional (osteoblastic/fibroblastic) OSs to control samples from healthy bone tissue (Supplementary Table S1). A total of 34 miRNAs were significantly deregulated ($P < 0.01$); of those, 11 had higher expression among the conventional OS group and 23 lower expression (Table 1, Fig. 1A). The most upregulated miRNAs in OS were *miR-181a* and *miR-181b*. *MiR-29b*, *miR-451*, and *miR-16* were among the most downregulated. Discrimination by profile between the 2 groups was strong. The cross-validation receiver operator characteristic (ROC) curve from the Bayesian compound covariate predictor had an area under the curve (AUC) of 0.986. This shows an extremely strong capacity for the relative expression levels of these 34 miRNAs to place a given sample into its correct group, OS or control.

For validation, we conducted qRT-PCR for a subset of the samples (Fig. 1B). Specifically, qRT-PCR confirmed differential expression for 9 of the 34 significant OS (shown in Fig. 1A) miRNAs among a random sampling of 7 specimens from OSs and 4 from controls. In particular, we confirmed the downregulation of *miR-29b*, *miR-16*, *miR-142-5p*, *miR-26b*, *let7g*, *miR-223*, and *miR-451* in OS samples as compared with controls. By contrast, *miR-181a* and *miR-181b* showed significant upregulation in OS cases (Fig. 1B). In addition, *miR-29a*, expressed from the same locus as *miR-29b*, was checked by qRT-PCR as a separate validation of the same locus. Other than 1 sample in each of 2 of the qRT-PCR experiments, all OS samples and control samples had distinct expression ranges, with no overlapping means.

Conventional, chondroblastic, and telangiectatic histologic subtypes of OS have distinct pathologic features. To interrogate the potential contribution of miRNA expression to the development of these different high-grade OS histologic subtypes, miRNA profiles from 18 conventional, 4 telangiectatic, 5 chondroblastic, 1 recurrent chondroblastic, 1 recurrent conventional, and 1 soft tissue OSs were subjected to unsupervised hierarchical clustering. Conventional, telangiectatic, chondroblastic, and even soft tissue OSs all clustered together in intermingled fashion (Fig. 1C). All 4 telangiectatic OSs clustered to 1 side of the highest hierarchy division, characterized

Published OnlineFirst February 20, 2012; DOI:10.1158/0008-5472.CAN-11-2663

Table 1. Differential expression of miRNAs in OS

Gene symbol	Fold change	Parametric *P*	FDR
A			
hsa-miR-181a	11.16	0.0000301	0.00128
hsa-miR-181b	5.35	0.003193	0.0611
*hsa-miR-10b**	4.36	0.0046651	0.0687
hsa-miR-7	4.12	0.0002834	0.0109
hsa-miR-214	4.11	0.0000223	0.00128
hsa-miR-190	4.04	0.0019492	0.0436
hsa-miR-181c	3.67	0.0063869	0.0895
*hsa-miR-616**	2.92	0.0068924	0.0895
hsa-miR-210	2.67	0.0023937	0.0483
hsa-miR-574-3p	2.26	0.0000037	0.000354
hsa-miR-487a	2.22	0.0045357	0.0687
hsa-miR-566	0.65	0.0072429	0.0895
hsa-miR-326	0.6	0.0045096	0.0687
hsa-miR-657	0.55	0.0046341	0.0687
hsa-miR-195	0.45	0.0015867	0.038
hsa-miR-483-3p	0.45	0.0072026	0.0895
hsa-miR-663	0.45	0.0099922	0.113
hsa-miR-150	0.41	0.0000002	0.0000766
hsa-miR-650	0.41	0.0020484	0.0436
hsa-let-7g	0.41	0.0092105	0.107
hsa-miR-519d	0.39	0.0034483	0.0629
*hsa-miR-16-2**	0.34	0.0003525	0.0122
hsa-miR-26b	0.33	0.0087029	0.104
hsa-miR-340	0.28	0.0000234	0.00128
hsa-miR-486-5p	0.26	0.0036685	0.0639
hsa-miR-126	0.24	0.0004251	0.0122
hsa-miR-488	0.23	0.0072343	0.0895
hsa-miR-335	0.22	0.0000286	0.00128
hsa-miR-16	0.2	0.0004448	0.0122
hsa-miR-451	0.2	0.0009	0.023
hsa-miR-29b	0.16	0.0000016	0.000306
*hsa-miR-126**	0.14	0.0004009	0.0122
hsa-miR-142-5p	0.1	0.0000029	0.000354
hsa-miR-223	0.064	0.0000058	0.000444
B			
*hsa-miR-181c**	1.75	0.02934	N/A
hsa-miR-27a	4.53	0.01469	N/A
C			
hsa-miR-15b	0.42	1.36E-05	N/A
hsa-miR-451	0.19	0.000422	N/A

NOTE: A, OS samples compared with control bone. The 34 genes are significant at the nominal 0.01 level of the univariate test; B, metastatic OSs compared with nonmetastatic OSs; C, chemoresistant OSs compared with chemosensitive.

by elevated expression of *miR-142-5p*, *miR-15a*, *miR-486-5p*, and *miR-488*. Small sample size makes statistical resolution of this finding unfeasible. Both conventional and chondroblastic OSs clustered with those 4 telangiectatic OSs. The overall coclustering of different subtypes suggests that with regard to miRNA expression, these tumors share more in common than not, which suggests that the miRNA expression represents more a shared oncogenic program than a differentiation profile alone, as these tumors are distinctly dissimilar in cell differentiation state. miRNA profiling therefore may not be helpful in defining histologically based OS subtype classifications.

To validate against an alternate data set, the publicly available S-MED database (19) was queried for the 34 miRNAs highlighted by our OS signature. The 15 OS samples (not subtyped) and 6 control bone samples recorded in the S-MED database had raw expression data for 26 of these miRNAs. Expression of 17 corroborated the differential expression in our samples (8 were significant with Student *t* test *P* values ranging from 0.006 to 5×10^{-8}.) These statistically significant and concordant expression data included higher expression of *miR-181c* and *miR-190* in S-MED OS specimens and lower expression of *miR-16*, *miR-126**, *miR-150*, *miR-195*, *miR-657*, and *miR-340*. Although the S-MED database includes fewer OS specimens than our primary data and lacks any clinical or pathologic annotation, it provides validation of the most important members of our OS miRNA signature profile from an alternate sample source and profiling platform.

miR-181b is inversely correlated with *miR-29b* in OS

To confirm deregulation of miRNA expression within tumor cells specifically, *in situ* hybridization of probes antisense to the differentially expressed *miR-181b* and *29b* was carried out with formalin-fixed, paraffin-embedded tissue sections processed from 9 of the same pretreatment biopsy specimens from which fresh tissue for total RNA isolation had been initially banked. As shown in Fig. 2, *in situ* hybridization with LNA-modified anti–*miR-181b* (panel B) or anti-*miR-29b* (panel C) probes showed results consistent with qRT-PCR (panel D). No signal was detected with scrambled oligo showing probe specificity (data not shown). Some tissues showed positive hybridization for the downregulated *miRNA-29b* (Fig. 2D). Although downregulation is not tantamount to absence, this nonetheless prompted further investigation. Using double labeling for *miR-29b* and *miR-181b*, it was confirmed that expression did not colocalize to the same cells (Fig. 2E, F), suggesting that the pro-osteoblast differentiation *miR-29b* was specifically absent in cells with the most robust oncogenic program of *miR-181b* expression. Additional *in situ* hybridization validation was carried out using a bone cancer tissue microarray (US Biomax, Inc.) that included 8 core tissue sections from 4 OSs. Two of the OS specimens showed strong staining for miR-181b and minimal miR-29b staining (data not shown), further evidence for miRNAs that may differentiate tumor versus normal bone.

miRNA expression signatures for OS metastasis and chemotherapeutic response

Ten OS patients either presented with or later developed clinically apparent metastatic disease. Their biologically aggressive tumors clustered together on unsupervised hierarchical clustering, loosely separate from the comparison 19 localized OSs (Fig. 3A). Differentially expressed miRNAs

Published OnlineFirst February 20, 2012; DOI:10.1158/0008-5472.CAN-11-2663

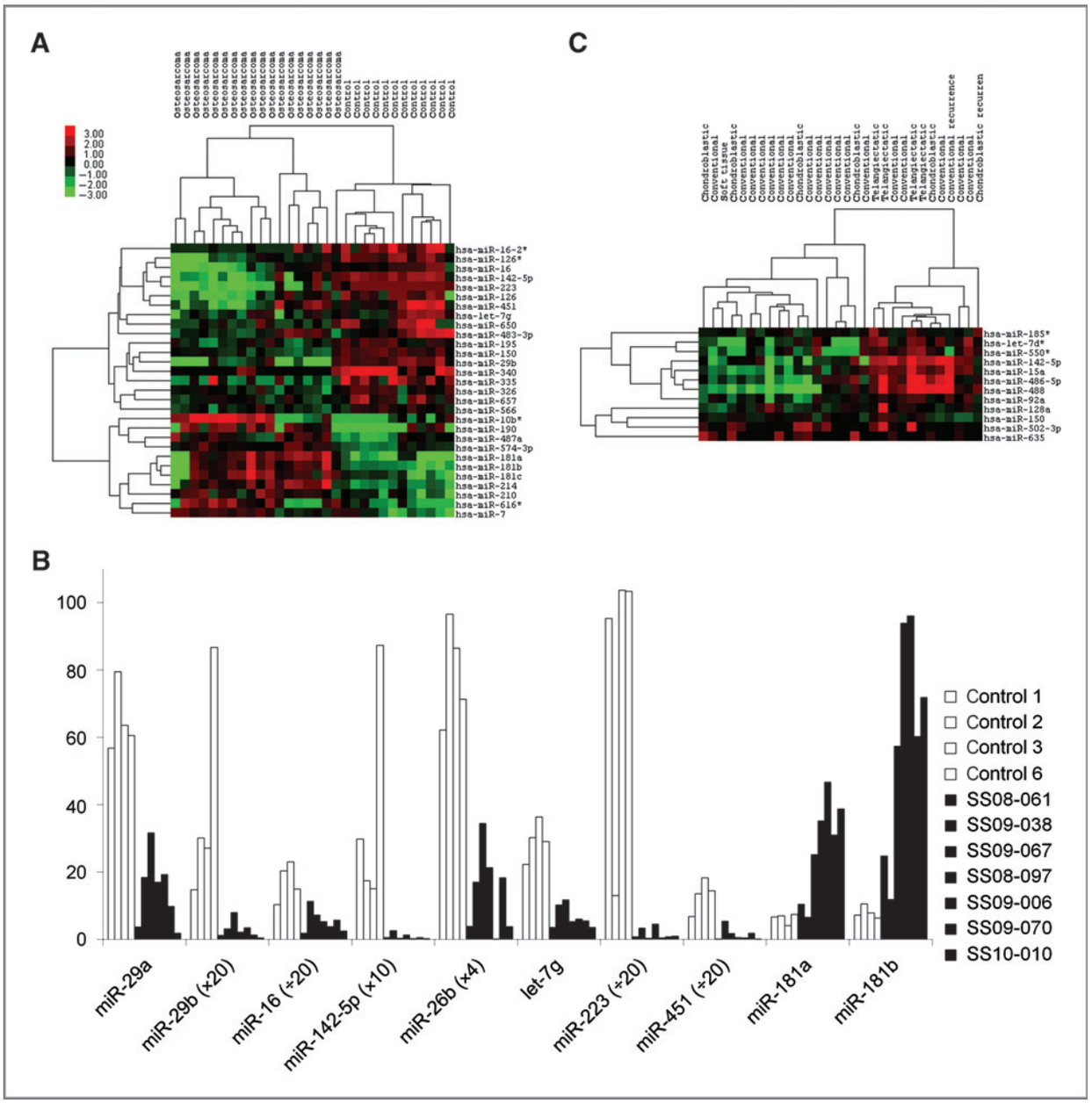

Figure 1. An miRNA expression signature for OS. A, unsupervised clustering of miRNA expression profiling from 18 pretreatment tumor total RNA obtained from conventional OSs in comparison with 12 normal bone tissues. B, quantitative RT-PCR confirmed differential expression for a subset of control and OS samples and a subset of highlighted miRNAs. C, unsupervised clustering of miRNA expression profiles from 30 pretreatment tumor total RNA samples of varied histologic subtypes, showing coclustering.

included 1.75- and 4.53-fold increased expression of *miR-181c** and *miR-27a*, respectively, in metastatic OSs. The class prediction analysis with these 2 miRNAs yielded a relatively strong ROC curve with an AUC of 0.805, indicating that the expression level of these 2 miRNAs alone discriminated between tumors that would and would not develop clinical metastases.

As OS patients typically receive chemotherapy after biopsy, but before resection, the percentage necrosis or treatment effect noted by the pathologist in the resection specimen has been found to be a powerful prognostic tool (20). All OS patients with pretreatment sample miRNA profiles available and who received neoadjuvant chemotherapy followed by resection and histopathologic grading of necrosis ($n = 27$, Supplementary Table S1), were analyzed for a correlation between differentially expressed pretreatment miRNAs and the percentage necrosis following chemotherapy. Spearman correlation, which measures the correlation of rank ordering between 2 values, identified expression of 8 miRNAs positively

Published OnlineFirst February 20, 2012; DOI:10.1158/0008-5472.CAN-11-2663

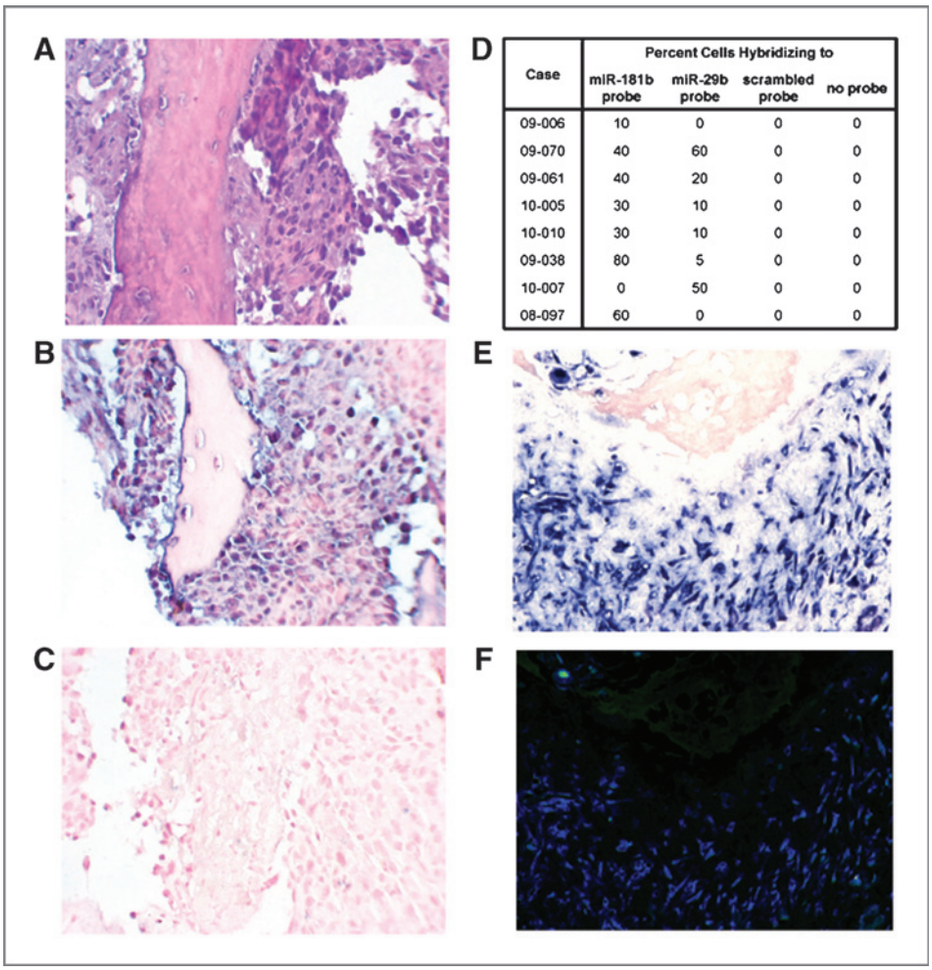

Case	Percent Cells Hybridizing to			
	miR-181b probe	miR-29b probe	scrambled probe	no probe
09-006	10	0	0	0
09-070	40	60	0	0
09-061	40	20	0	0
10-005	30	10	0	0
10-010	30	10	0	0
09-038	80	5	0	0
10-007	0	50	0	0
08-097	60	0	0	0

Figure 2. Validation by *in situ* hybridization. Formalin-fixed, paraffin-embedded tissues from the same biopsies that rendered the total RNA samples were sectioned and stained with hematoxylin and eosin (A) or probed with antisense oligonucleotides against *miR-181b* (B) or *miR-29b* (C). The percentage of cells hybridizing to the tested probes were generated from counting 10 high powered fields (D). Samples with both *miR-181* and *miR-29b* hybridization were subjected to cohybridization with differentially labeled detection systems, showing little to no overlap in positive cells (*miR-29b* stained red in E and fluorescent green in F, *miR-181* stained blue in E and fluorescent blue in F).

correlated with percentage necrosis at less than 0.01 stringency and 1 negatively correlated (Supplementary Table S2A; Fig. 3B shows unsupervised clustering by Spearman-identified miRNAs). Pearson correlation, which identifies linear relationships rather than rankings, identified 7 miRNAs positively correlated with necrosis at less than 0.01 stringency (Supplementary Table S2B; Fig. 3C shows unsupervised clustering by Pearson-identified miRNAs). *miR-451* and *miR-15b*, with the 2 highest Spearman correlation coefficients of 0.64 and 0.619, respectively, were also highlighted by the Pearson correlation list, having correlation coefficients of 0.533 and 0.539, respectively. Thus, increased expression of *miR-15b* (from the *miR-15/16* family) and *miR-451* in pretreatment samples was the most stringent predictor of good response to chemotherapy. RT-PCR validated expression levels of *miR-451* and *miR-15b* in a subset of chemosensitive and chemoresistant OS samples (Supplementary Fig. S1).

Functional validation of *miR-16* as tumor suppressive and miR-27a as prometastatic in OS cells

To determine the functional relevance of miRNA deregulation in OS, we studied the effect of *miR-16* and *miR-27a* manipulation on OS cells. We first checked the endogenous *miR-16* and *miR-27a* levels by qRT-PCR in 1 human osteoblast and 6 human OS cell lines. Three OS cell lines (HOS, KHOS, and U2OS) exhibited significantly low levels of *miR-16* as compared with hOB (Supplementary Fig. S2). Similarly, *miR-27a* expression levels were lower in these cells while the MG-63 cells, capable of metastasis and the highly metastatic LM-7 cells displayed higher levels (Supplementary Fig. S2).

Next, we set to determine whether reintroduction of these miRs affected the tumorigenic traits of OS cells (Supplementary Fig. S3 and S4). Using XTT test, we observed significant growth inhibition in U2OS and hOB cells (Supplementary Fig. S5). In contrast, we did not detect this effect in HOS, KHOS, and SaOS2 cells (Fig. 4A, Supplementary Fig. S5). Nevertheless, overexpression of *miR-16* in OS cells displaying low levels of endogenous *miR-16* was associated with significant reduction in colony formation ability (Fig. 4B and Supplementary Fig. S5). Moreover, HOS-expressing *miR-16* displayed increased apoptosis in the presence of doxorubicin (Fig. 4C).

We next evaluated the tumor suppressor function of *miR-16 in vivo*. HOS cells overexpressing control *miR* or *miR-16* were

Published OnlineFirst February 20, 2012; DOI:10.1158/0008-5472.CAN-11-2663

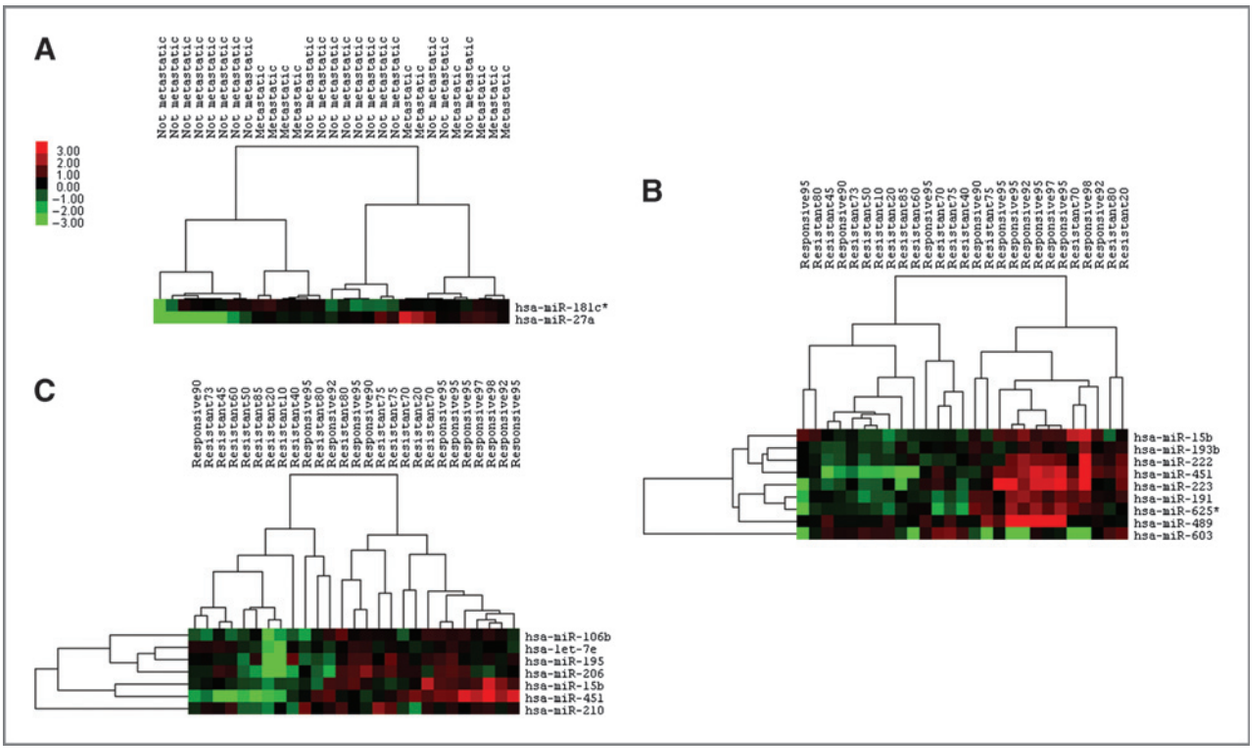

Figure 3. miRNA expression profiling identifies behavioral subgroups of OS. A, unsupervised clustering according to expression of miRNAs differentially expressed in pretreatment samples from OSs that present or develop clinical metastasis or remain clinical localized through treatment and follow-up. B, unsupervised hierarchical clustering of OSs according to their pretreatment expression of miRNAs that correlate by Spearman correlation coefficient with percentage necrosis following neoadjuvant chemotherapy. C, unsupervised hierarchical clustering of OSs according to their pretreatment expression of miRNAs that correlate by Pearson correlation coefficient with percentage necrosis following neoadjuvant chemotherapy.

xenografted into the flanks of NOD/SCID mice and monitored for tumor formation. We found that overexpressing *miR-16* produced tumors of smaller volume and smaller final mass (Fig. 4D–F). Furthermore, *miR-16* overexpressing HOS xenografts exhibited increased activated caspase-3 staining (Fig. 4G), an indicator of enhanced apoptosis in the absence of cytotoxic treatment.

To interrogate the impact of *miR-27a* overexpression on the metastatic potential of OS cells, we infected HOS cells with a lentiviral vector that expresses either *miR-27a* or control miR along with a GFP reporter. *In vitro*, a wound healing assay found increased migration with overexpression of *miR-27a* versus control miR (Fig. 4H). Similarly, Matrigel invasion assay showed that *miR-27a* increased invasiveness (Fig. 4I). *miR-27a*–expressing cells were next injected i.v. into NOD/SCID mice to evaluate the metastatic potential of these cells. Six weeks later, the animals were scarified and dissected to look for both microscopic and macroscopic metastases. We found that overexpression of *miR-27a* is associated with increased ability to form metastatic foci compared with control miR. The number and size of pulmonary metastases was significantly increased as well as the presence of macroscopic metastatic disease in the bones of the legs and forearms (Fig. 4J–N). Additional functional validation in other cell lines confirmed promigration and invasion effects of *miR-27a* (Supplementary Fig. S5).

Predicted targets of differentially expressed miRNAs reflected in OS

MiRNAs are known to have downregulatory effects at the level of transcript longevity and translational control. Expression levels of TargetScan-predicted target genes of *miR-16* were found to be reduced in OS and osteoblast cell lines following overexpression of *miR-16* (Fig. 5A). Similarly, expression levels of predicted target genes of *miR-27a* were found to be reduced in OS cell lines following overexpression of *miR-27a* (Fig. 5B).

We expanded the analysis of expression of target genes by profiling gene expression by Affymetrix array in 14 of the OS samples in our cohort and 4 of the normal bone control samples. Our data revealed differential changes in a significant number of genes (data not shown). The miRNA and mRNA expression profiles were then integrated to identify functional relationships that may contribute to OS. Instead of correlating gene expression with all miRNAs, we focused on miRNAs in which differential expression was most significant in OS; *miR-16*, *miR-142-5p*, *miR-29b* as downregulated miRNAs in OS and *miR-181* and *miR-27a* as upregulated miRNAs in OS. Positive and negative correlations were found. However, we focused on the differentially expressed genes that followed the directional change predicted by the miRNA; increased expression in OS for genes targeted by *miR-16*, *miR-142-5p*, and *miR-29b* and decreased expression of genes targeted by *miR-181* and *miR-27a* (Supplementary Tables S3A and S3B). We found that

Published OnlineFirst February 20, 2012; DOI:10.1158/0008-5472.CAN-11-2663

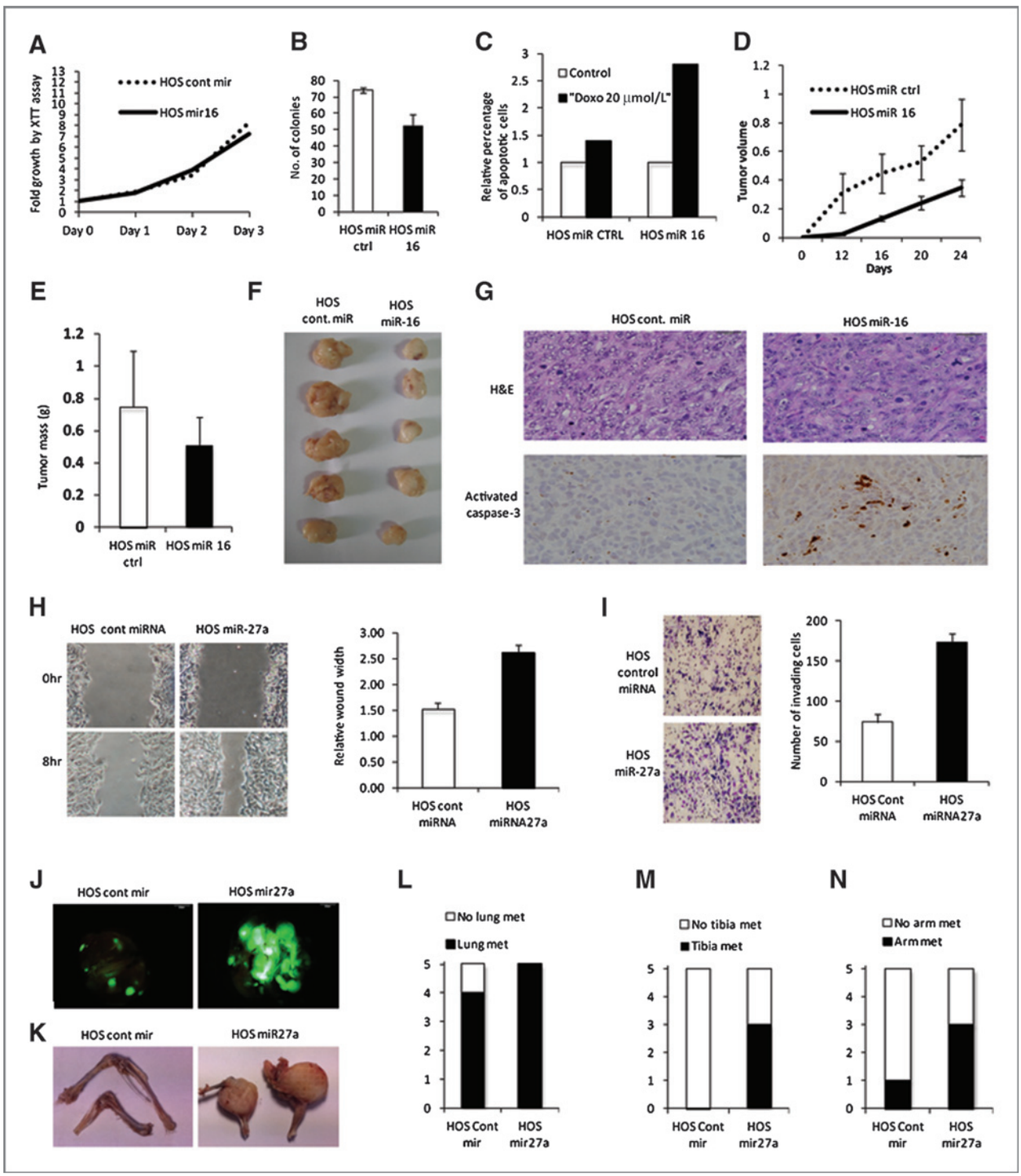

Figure 4. Functional validation of *miR-16* and *miR-27a* in the HOS OS cell line. A, XTT assay shows no significant proliferative effect of *miR-16* overexpression by lentivirus, compared with scrambled miR control. B, assessment of colony formation confirms tumor-suppressive role for *miR-16*. C, apoptotic response following exposure to doxorubicin shows a chemosensitizing role. D. HOS-*miR-16* or control cells were injected s.c. into the flanks of NOD-SCID mice; tumor volume (cm^3) was assessed every week. E, tumor mass (in grams) was measured at the end of the experiment. F, representative tumor masses excised from mice. G, H&E staining and activated caspase-3 immunohistochemistry on paraffin-embedded sections of representative tumors (brown color indicates act. Casp3 positivity). H, migration assay (wound healing) of HOS-*miR-27a* or control cells monitored in serum-free media for 8 hours. I, Matrigel invasion assay of HOS-*miR27a* and control cells monitored using Boyden chambers. J, HOS-*miR-27a* or control cells were injected i.v. into the tail vein of NOD/SCID mice and microscopic and macroscopic metastasis assessed at 6-weeks by GFP fluorescence in the lungs. K, representative pictures of the forearms and tibias of the same animals. L–N, quantification of the metastasis positive animals in the indicated organs. H&E: hematoxylin and eosin.

Published OnlineFirst February 20, 2012; DOI:10.1158/0008-5472.CAN-11-2663

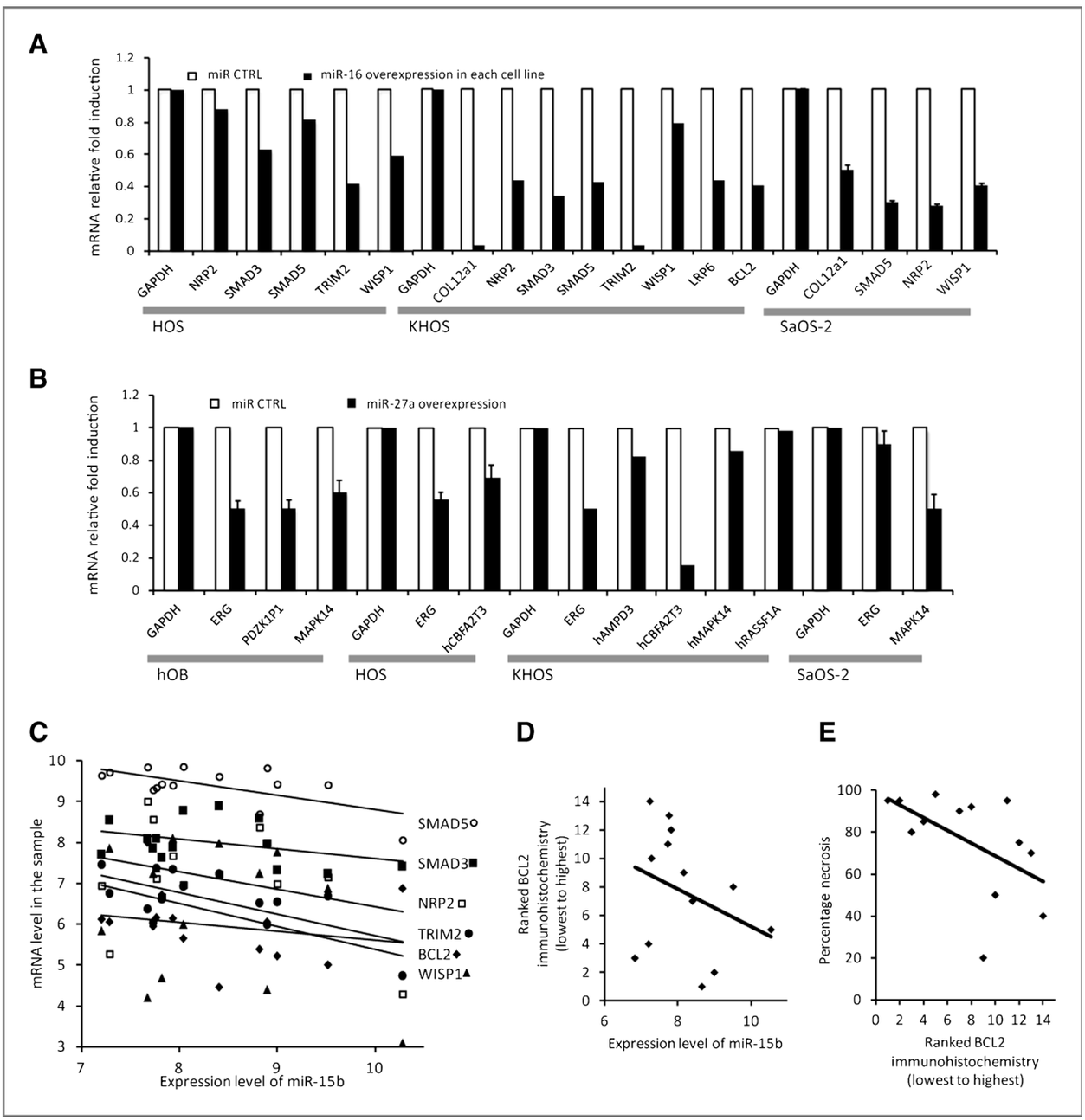

Figure 5. Predicted targets respond to miR expression levels. A, HOS, KHOS, and SaOS-2 OS cell lines stably transfected by lentivirus with an overexpression vector of *miR-16* or scrambled miR control showed reduced levels of TargetScan predicted target genes by qRT-PCR. B, functional validation of *miR-27a* versus scrambled control miR in osteoblasts and OS cell lines show downregulation of TargetScan predicted target gene mRNAs, shown here by qRT-PCR. C, the Affymetrix array expression level of these same predicted *miR-15/16* family targets are plotted against *miR-15b* levels by sample and each linear regression follows the expected correlation direction. D, blindly ranked BCL2 protein levels ascertained by immunohistochemistry correlate even more strongly than transcript levels with *miR-15b* levels by specimen. E, this BCL2 immunohistochemical ranking also correlates with the predicted chemoresponsiveness of tumors.

several known OS genes are indeed targeted by these different miRNA classes. Gene ontologies and Kegg pathways analyses of these predicted target genes highlighted significant changes in transcriptional regulation, cell-cycle control, and known cancer signaling pathways (Table 2 and Supplementary Tables S4 and S5).

To further investigate 1 miRNA as an example, *miR-15b* from the *miR-15/16* family was selected due to the fact that it showed differential expression within the cohort of OSs and predicted chemosensitivity. The expression level of *miR-15b* from each specimen was plotted against the Affymetrix mRNA level in the same sample for 6 of the prominent differentially expressed

Published OnlineFirst February 20, 2012; DOI:10.1158/0008-5472.CAN-11-2663

Table 2. Kegg pathway analysis of Target Scan predicted target genes of *miR-16*, *miR-142-5p*, and *miR-29b* that were confirmed to have increased expression in OSs by affymetrix cDNA profiling

Kegg pathway term	Gene count	Fold enrichment	*P*
Pathways in cancer	29	3.5	6.64×10^{-09}
Focal adhesion	26	5.1	1.65×10^{-11}
Small cell lung cancer	16	7.5	1.72×10^{-09}
Regulation of actin cytoskeleton	16	2.9	3.11×10^{-04}
ECM–receptor interaction	14	6.5	1.33×10^{-07}
Neurotrophin signaling pathway	14	4.4	1.23×10^{-05}
Axon guidance	14	4.2	1.90×10^{-05}
Wnt signaling pathway	11	2.8	0.004713
Ubiquitin-mediated proteolysis	10	2.9	0.007635
Colorectal cancer	9	4.2	0.001193
T-cell receptor signaling pathway	9	3.3	0.005802
Glioma	8	5.0	9.75×10^{-04}
Melanoma	8	4.4	0.001982
Pancreatic cancer	8	4.3	0.002149
Chronic myeloid leukemia	8	4.2	0.00272
TGF-β signaling pathway	8	3.6	0.006232
Prostate cancer	8	3.5	0.007049
Renal cell carcinoma	7	3.9	0.008248

NOTE: Genes in each pathway are shown in Supplementary Table S4 (A shows the Gene Ontology groups and B identifies Kegg pathway–specific genes.)

genes that are predicted targets and responsive in cell line experiments (Fig. 5C). A linear regression trend line for each series showed the predicted direction of correlation with increasing level of *miR-15b* linked to decreasing levels of each gene's mRNA.

Because miRNAs can have more profound effects on translation than transcription, we carried out immunohistochemistry in tissue sections from a subset of the OS samples. We selected 2 genes, one a well-known gene in OS, *BCL2*, the other a gene not previously associated with OS, but also a target of the *miR-15/16* family, *NFAT5*. For both, immunohistochemistry confirmed increased protein presence in the cohort OSs than in the osteoblasts of bone marrow controls (Supplementary Fig. S6). The BCL2 immunohistochemically stained sections were blindly ranked from least to most positive for staining. This ranking was then plotted against the expression level of *miR-15b* (Fig. 5D) and against the expected clinical parameter of percentage necrosis as measured from later resection surgery to quantify chemoresponsiveness (Fig. 5E). Linear regressions strongly followed the expected correlation in each. Although these correlations only consider 1 example, they suggest that the differentially expressed miRNAs play a direct role in controlling transcript levels and translational success of predicted target genes in OS.

Discussion

We report unique OS signatures of miRNA expression related to the OS character and pathogenesis, to clinical metastasis, and to chemotherapy response. The deregulation of *miR-181b* specifically in the malignant cells in OS tissues by *in situ* hybridization provides a potential OS marker. Furthermore, *miR-181b* and *miR-29b* expression inversely correlate in subpopulations of cells in the tumors. Significantly, our *in vitro* and *in vivo* functional experiments validate *miR-16* as a tumor suppressor and *miR-27a* as prometastatic in OS and osteoblast cell lines. These data suggest potential targets for future therapeutic strategies. Furthermore, our study indicates that by correlating genome-wide gene and miRNA expression profiles, putative functional miRNA–mRNA interactions could be identified in OS.

The conventional OS miRNA expression signature we report here, showed strong statistical significance even in a relatively small sample size. This suggests profile consistency across the samples. Given the genetic and cytogenetic complexity inherent to OS (2), this consistency raises the possibility that miRNAs play a central role in osteosarcomagenesis. That the miRNA profile differed little even among histologically disparate samples from chondroblastic and telangiectatic OSs further suggests a role for these miRNAs in development of OS generally. Validation against another patient group confirmed the differential expression of the critical members of this (19). A final validation of our signature derives from our observation that some of the prominent signature miRNAs are also highlighted by OS metastasis and chemotherapy responsiveness signatures (Supplementary Fig. S7).

As we qualitatively evaluate these signature OS miRNAs, downregulated miRNAs are most striking. *MiR-29b* figured prominently in this list. We also showed its localization to a distinct cell subpopulation within the tumors. This fits the

Published OnlineFirst February 20, 2012; DOI:10.1158/0008-5472.CAN-11-2663

powerful role of *miR-29b* as a prodifferentiation miRNA in normal osteoblasts (21). Other signature downregulated miRNAS have known prodifferentiation roles in other tissues, *miR-223* in myeloid (22) and *miR-451* in erythroid differentiation (23). *miR-29b* is also known as a tumor suppressor miRNA (24). The tumor suppressor category also encompasses other prominently downregulated members of the signature profile, including *miR-142-5p* (25), *miR-340* (26), breast cancer metastasis suppressing *miR-335* (27), *BCL-2* targeting *miR-16/16-2** (reviewed in ref. 28), *miR-126/126** (reviewed in ref. 29), and *miR-195* (30), an *miR-15/16*-related miRNA. Together with our *in vitro* functional validation for *miR-16*, these findings highlight critical tumor suppressor functions of the *miR-15/16* family in OS.

Most upregulated miRNAs in the OS signature are known as oncomiRs, such as *miR-190* (31), *miR-10b* [(32) and references therein], *miR-7* [(33) and references therein], *miR-214* [(34) and references therein], and *miR-210* (35). Although *miR-574-3p* is not well characterized in the literature, it is predicted to target disabled homolog 2 interacting protein, which is silenced in a number of cancers (36–38), retinoid X receptor alpha, which is associated with vitamin D metabolism and polymorphism-based cancer risk (39), and FOS-like antigen 2 (*Fosl2/Fra2*), which is a prodifferentiation gene in osteoblasts (40). Most prominently, 3 of the 4 miRNAs from the *miR-181* group were highly upregulated in OS samples. *miR-181* has been associated with stemness and poor prognosis in other cancers [(41) and references therein]. Furthermore, *miR-181* activates *Wnt* signaling (42), important in OS pathogenesis (43). Together with our *in situ* hybridization confirmation that *miR-181* identifies a subgroup of cells within OS tissues that lack *miR-29b*–driven differentiation, these data highlight *miR-181* as a critical OS oncomiR.

Increased expression of *miR-181c** and *miR-27a* at pretreatment biopsy was found to be prognostic of metastatic disease. This punctuates the importance of the *miR-181* family to OS. *miR27a* is a known oncomiR, associated with metastasis in gastric cancer (44) and poor prognosis in ovarian carcinoma (45). Our *in vitro* and *in vivo* experiments confirmed that *miR-27a* overexpression enhances migration, invasion, and proliferation in metastatic sites. These findings correlate with the recently described inhibition of osteoblast differentiation by *miR-27a* (18). Targeted therapies against *miR-27a* are emerging (46, 47).

Expression levels of *miR-451* and *miR-15b* in pretreatment specimens both correlated positively with percentage necrosis following neoadjuvant chemotherapy. Reduced expression of *miR-451* was also prominent in the general OS signature. Although *miR-15b* itself was not highlighted in the general OS signature, *miR-16, miR16-2**, and *miR-195*, all from the same *miR-15/16* family, were. Apparently, reduced expression of these miRNAs characterizes OS generally, but among OSs, further reduced expression correlates with resistance to chemotherapy. *MiR-15b* and other family members target Bcl-2, which could explain their downregulation in chemoresistant tumors (48). We confirmed by immunohistochemistry the increased presence of BCL-2 in the OS histologic specimens compared with controls. Furthermore, increased apoptosis was identified both in untreated xenografts and doxorubicin-treated cultures of OS cells driven to overexpress *miR-16*. Our findings did not corroborate any of the specific miRNAs reported to predict chemotherapeutic response in a series of formalin-fixed, paraffin-embedded OS specimens (10). This other study differed in source and method of RNA isolation. It also focused on ifosfamide, an infrequent neoadjuvant chemotherapy for OS in the United States and received by only one of our patients. Furthermore, our findings did not highlight any of the previously investigated individual miRNAs noted to have roles in OS cell lines (6–9).

The profound effects of *miR-16, miR-142-5p, miR-29b, miR-181,* and *miR-27a* on the microarray-defined expression of their predicted target genes, with statistically significant differences in the predicted direction, suggest that these miRNAs play central roles in defining the expression identity of OS. Our study reveals many potential functional miRNA–mRNA relationships that will need to be further explored mechanistically for their involvement in OS pathogenesis. Gain and loss of function studies are needed to investigate further the role of these miRNAs that have correlated with transcriptional regulation, cell-cycle control, and known cancer signaling pathways. Finally, the discovery of previously unidentified functional relationships may lead to the development of novel therapeutic approaches. Further investigation into the potentially more poignant effects on translation of their targets may yield additional insights into this newly recognized method of an OS cell defining itself.

Making clear sense of how the genetic chaos that defines OS derives such a patterned clinical disease remains a distant goal, but these data strongly recommend the pursuit of osteosarcomiRs and silenced OS tumor suppressor miRNAs as critically associated with development of OS. The statistical strength of the OS signature we report, the consistency across multiple histologic subtypes, and especially the overlap of the general OS signature with signatures predictive of metastasis and predictive of response to chemotherapy, all highlight the central role of these dysregulated miRNAs in osteosarcomagenesis. Our validation studies for key signature OS miRNAs and integration of miRNA expression with mRNA expression, together with existing literature provide models for future study.

Disclosure of Potential Conflicts of Interest

No potential conflicts of interest were disclosed.

Acknowledgments

The authors thank Saleh Khwaled and Suhaib Abdeen from Hebrew University for assistance with mice work; John J. Wixted from the University of Massachusetts, Worcester, for assistance in procuring control bone specimens; David LaPointe, also from the University of Massachusetts, Worcester, for assistance with bioinformatics analysis; and Huifeng Jin and Mohamed Salama from the University of Utah for assistance with immunohistochemistry.

Grant Support

This work was supported, in part, by the Alex's Lemonade Stand Foundation (ALSF) "A" Award to R.I. Aqeilan, and Israeli Cancer Research Funds (ICRF) to R.I. Aqeilan and Z. Salah. K.B. Jones is supported by the NIH

Published OnlineFirst February 20, 2012; DOI:10.1158/0008-5472.CAN-11-2663

K08CA138764 and the Huntsman Cancer Foundation. R.L. Randall is supported by the Huntsman Cancer Foundation. G.S. Stein and J.B. Lian are supported by NIH/NIAMS AR039588-19. S. Volinia is supported by AIRC (IG 8588) and PRIN MIUR 2008.

The costs of publication of this article were defrayed in part by the payment of page charges. This article must therefore be hereby marked *advertisement* in accordance with 18 U.S.C. Section 1734 solely to indicate this fact.

Received August 10, 2011; revised December 14, 2011; accepted January 7, 2012; published OnlineFirst February 20, 2012.

References

1. Ottaviani G, Jaffe N. The epidemiology of osteosarcoma. Cancer Treat Res 2009;152:3–13.
2. Gorlick R. Current concepts on the molecular biology of osteosarcoma. Cancer Treat Res 2009;152:467–78.
3. Bacci G, Bertoni F, Longhi A, Ferrari S, Forni C, Biagini R, et al. Neoadjuvant chemotherapy for high-grade central osteosarcoma of the extremity. Histologic response to preoperative chemotherapy correlates with histologic subtype of the tumor. Cancer 2003; 97:3068–75.
4. Lewis BP, Burge CB, Bartel DP. Conserved seed pairing, often flanked by adenosines, indicates that thousands of human genes are microRNA targets. Cell 2005;120:15–20.
5. Croce CM. Causes and consequences of microRNA dysregulation in cancer. Nat Rev Genet 2009;10:704–14.
6. Ziyan W, Shuhua Y, Xiufang W, Xiaoyun L. MicroRNA-21 is involved in osteosarcoma cell invasion and migration. Med Oncol 2011;28: 1469–74.
7. Zhang H, Cai X, Wang Y, Tang H, Tong D, Ji F. microRNA-143, down-regulated in osteosarcoma, promotes apoptosis and suppresses tumorigenicity by targeting Bcl-2. Oncol Rep 2010;24:1363–9.
8. Song B, Wang Y, Xi Y, Kudo K, Bruheim S, Botchkina GI, et al. Mechanism of chemoresistance mediated by miR-140 in human osteosarcoma and colon cancer cells. Oncogene 2009;28: 4065–74.
9. He C, Xiong J, Xu X, Lu W, Liu L, Xiao D, et al. Functional elucidation of MiR-34 in osteosarcoma cells and primary tumor samples. Biochem Biophys Res Commun 2009;388:35–40.
10. Gougelet A, Pissaloux D, Besse A, Perez J, Duc A, Dutour A, et al. Micro-RNA profiles in osteosarcoma as a predictive tool for ifosfamide response. Int J Cancer 2010;129:680–90.
11. Randall RL, Wade M, Albritton K, Joyner D. Retrieval yield of total and messenger RNA in mesenchymal tissue *ex vivo*. Clin Orthop Relat Res 2003; Oct (415):59–63.
12. Liu CG, Calin GA, Volinia S, Croce CM. MicroRNA expression profiling using microarrays. Nat Protoc 2008;3:563–78.
13. Simon R, Lam A, Li MC, Ngan M, Menenzes S, Zhao Y. Analysis of gene expression data using BRB-ArrayTools. Cancer Inform 2007; 3:11–7.
14. Bartel DP. MicroRNAs: genomics, biogenesis, mechanism, and function. Cell 2004;116:281–97.
15. Shi R, Chiang VL. Facile means for quantifying microRNA expression by real-time PCR. Biotechniques 2005;39:519–25.
16. Valeri N, Gasparini P, Fabbri M, Braconi C, Veronese A, Lovat F, et al. Modulation of mismatch repair and genomic stability by miR-155. Proc Natl Acad Sci U S A 2010;107:6982–7.
17. Nuovo GJ, Elton TS, Nana-Sinkam P, Volinia S, Croce CM, Schmittgen TD. A methodology for the combined *in situ* analyses of the precursor and mature forms of microRNAs and correlation with their putative targets. Nat Protoc 2009;4:107–15.
18. Hassan MQ, Gordon JA, Beloti MM, Croce CM, van Wijnen AJ, Stein JL, et al. A network connecting Runx2, SATB2, and the miR-23a∼27a∼24-2 cluster regulates the osteoblast differentiation program. Proc Natl Acad Sci U S A 2010;107:19879–84.
19. Sarver AL, Phalak R, Thayanithy V, Subramanian S. S-MED: sarcoma microRNA expression database. Lab Invest 2010;90:753–61.
20. Glasser DB, Lane JM, Huvos AG, Marcove RC, Rosen G. Survival, prognosis, and therapeutic response in osteogenic sarcoma. The Memorial Hospital experience. Cancer 1992;69:698–708.
21. Li Z, Hassan MQ, Jafferji M, Aqeilan RI, Garzon R, Croce CM, et al. Biological functions of miR-29b contribute to positive regulation of osteoblast differentiation. J Biol Chem 2009;284:15676–84.
22. Vasilatou D, Papageorgiou S, Pappa V, Papageorgiou E, Dervenoulas J. The role of microRNAs in normal and malignant hematopoiesis. Eur J Haematol 2010;84:1–16.
23. Patrick DM, Zhang CC, Tao Y, Yao H, Qi X, Schwartz RJ, et al. Defective erythroid differentiation in miR-451 mutant mice mediated by 14–3-3zeta. Genes Dev 2010;24:1614–9.
24. Eyholzer M, Schmid S, Wilkens L, Mueller BU, Pabst T. The tumour-suppressive miR-29a/b1 cluster is regulated by CEBPA and blocked in human AML. Br J Cancer 2010;103:275–84.
25. Sempere LF, Liu X, Dmitrovsky E. Tumor-suppressive microRNAs in lung cancer: diagnostic and therapeutic opportunities. Scientific World J 2009;9:626–8.
26. Guled M, Lahti L, Lindholm PM, Salmenkivi K, Bagwan I, Nicholson AG, et al. CDKN2A, NF2, and JUN are dysregulated among other genes by miRNAs in malignant mesothelioma—a miRNA microarray analysis. Genes Chromosomes Cancer 2009;48:615–23.
27. Tavazoie SF, Alarcon C, Oskarsson T, Padua D, Wang Q, Bos PD, et al. Endogenous human microRNAs that suppress breast cancer metastasis. Nature 2008;451:147–52.
28. Aqeilan RI, Calin GA, Croce CM. miR-15a and miR-16–1 in cancer: discovery, function and future perspectives. Cell Death Differ 2010;17: 215–20.
29. Meister J, Schmidt MH. miR-126 and miR-126*: new players in cancer. ScientificWorld J 2010;10:2090–100.
30. Liu L, Chen L, Xu Y, Li R, Du X. microRNA-195 promotes apoptosis and suppresses tumorigenicity of human colorectal cancer cells. Biochem Biophys Res Commun 2010;400:236–40.
31. Zhang Y, Li M, Wang H, Fisher WE, Lin PH, Yao Q, et al. Profiling of 95 microRNAs in pancreatic cancer cell lines and surgical specimens by real-time PCR analysis. World J Surg 2009;33:698–709.
32. Ma L, Reinhardt F, Pan E, Soutschek J, Bhat B, Marcusson EG, et al. Therapeutic silencing of miR-10b inhibits metastasis in a mouse mammary tumor model. Nat Biotechnol 2010;28:341–7.
33. Chou YT, Lin HH, Lien YC, Wang YH, Hong CF, Kao YR, et al. EGFR promotes lung tumorigenesis by activating miR-7 through a Ras/ERK/Myc pathway that targets the Ets2 transcriptional repressor ERF. Cancer Res 2010;70:8822–31.
34. Qiang R, Wang F, Shi LY, Liu M, Chen S, Wan HY, et al. Plexin-B1 is a target of miR-214 in cervical cancer and promotes the growth and invasion of HeLa cells. Int J Biochem Cell Biol 2011;43:623–41.
35. Zhang Z, Sun H, Dai H, Walsh RM, Imakura M, Schelter J, et al. MicroRNA miR-210 modulates cellular response to hypoxia through the MYC antagonist MNT. Cell Cycle 2009;8:2756–68.
36. Yano M, Toyooka S, Tsukuda K, Dote H, Ouchida M, Hanabata T, et al. Aberrant promoter methylation of human DAB2 interactive protein (hDAB2IP) gene in lung cancers. Int J Cancer 2005;113:59–66.
37. Qiu GH, Xie H, Wheelhouse N, Harrison D, Chen GG, Salto-Tellez M, et al. Differential expression of hDAB2IPA and hDAB2IPB in normal tissues and promoter methylation of hDAB2IPA in hepatocellular carcinoma. J Hepatol 2007;46:655–63.
38. Xie D, Gore C, Liu J, Pong RC, Mason R, Hao G, et al. Role of DAB2IP in modulating epithelial-to-mesenchymal transition and prostate cancer metastasis. Proc Natl Acad Sci U S A 2010;107:2485–90.
39. Karami S, Brennan P, Navratilova M, Mates D, Zaridze D, Janout V, et al. Vitamin d pathway genes, diet, and risk of renal cell carcinoma. Int J Endocrinol 2010;2010:879362.
40. Bozec A, Bakiri L, Jimenez M, Schinke T, Amling M, Wagner EF. Fra-2/AP-1 controls bone formation by regulating osteoblast differentiation and collagen production. J Cell Biol 2010;190:1093–106.
41. Wang Y, Yu Y, Tsuyada A, Ren X, Wu X, Stubblefield K, et al. Transforming growth factor-beta regulates the sphere-initiating stem cell-

Published OnlineFirst February 20, 2012; DOI:10.1158/0008-5472.CAN-11-2663

like feature in breast cancer through miRNA-181 and ATM. Oncogene 2011;30:1470–80.
42. Qin L, Chen Y, Niu Y, Chen W, Wang Q, Xiao S, et al. A deep investigation into the adipogenesis mechanism: profile of microRNAs regulating adipogenesis by modulating the canonical Wnt/beta-catenin signaling pathway. BMC Genomics 2010;11:320.
43. Guo Y, Zi X, Koontz Z, Kim A, Xie J, Gorlick R, et al. Blocking Wnt/LRP5 signaling by a soluble receptor modulates the epithelial to mesenchymal transition and suppresses met and metalloproteinases in osteosarcoma Saos-2 cells. J Orthop Res 2007;25:964–71.
44. Katada T, Ishiguro H, Kuwabara Y, Kimura M, Mitui A, Mori Y, et al. microRNA expression profile in undifferentiated gastric cancer. Int J Oncol 2009;34:537–42.
45. Eitan R, Kushnir M, Lithwick-Yanai G, David MB, Hoshen M, Glezerman M, et al. Tumor microRNA expression patterns associated with resistance to platinum based chemotherapy and survival in ovarian cancer patients. Gynecol Oncol 2009;114:253–9.
46. Sun Q, Cong R, Yan H, Gu H, Zeng Y, Liu N, et al. Genistein inhibits growth of human uveal melanoma cells and affects microRNA-27a and target gene expression. Oncol Rep 2009;22:563–7.
47. Chintharlapalli S, Papineni S, Abdelrahim M, Abudayyeh A, Jutooru I, Chadalapaka G, et al. Oncogenic microRNA-27a is a target for anticancer agent methyl 2-cyano-3,11-dioxo-18beta-olean-1,12-dien-30-oate in colon cancer cells. Int J Cancer 2009;125:1965–74.
48. Xia L, Zhang D, Du R, Pan Y, Zhao L, Sun S, et al. miR-15b and miR-16 modulate multidrug resistance by targeting BCL2 in human gastric cancer cells. Int J Cancer 2008;123:372–9.